

CD20 and CD37 antibodies synergize to activate complement by Fc-mediated clustering

Simone C. Oostindie,^{1,2} Hilma J. van der Horst,³ Margaret A. Lindorfer,⁴ Erika M. Cook,⁴ Jillian C. Tupitza,⁴ Clive S. Zent,⁵ Richard Burack,⁵ Karl R. VanDerMeid,⁵ Kristin Strumane,¹ Martine E. D. Chamuleau,³ Tuna Mutis,³ Rob N. de Jong,¹ Janine Schuurman,¹ Esther C. W. Breij,¹ Frank J. Beurskens,¹ Paul W. H. I. Parren^{2,6} and Ronald P. Taylor⁴

¹Genmab, Utrecht, the Netherlands; ²Department of Immunohematology and Blood Transfusion, Leiden University Medical Center, Leiden, the Netherlands; ³Department of Hematology, Amsterdam University Medical Center, Amsterdam, the Netherlands; ⁴Department of Biochemistry and Molecular Genetics, University of Virginia School of Medicine, Charlottesville, Virginia, USA; ⁵Wilmot Cancer Institute, University of Rochester Medical Center, Rochester, NY, USA and ⁶Lava Therapeutics, Utrecht, the Netherlands

©2019 Ferrata Storti Foundation. This is an open-access paper. doi:10.3324/haematol.2018.207266

Received: October 2, 2018.

Accepted: February 19, 2019.

Pre-published: February 21, 2019.

Correspondence: *SIMONE C. OOSTINDIE* - sio@genmab.com

RONALD P. TAYLOR - rpt@virginia.edu

Supplementary Appendix for

CD20 and CD37 antibodies synergize to activate complement by Fc-mediated clustering

Simone C. Oostindie,^{1,2,†} Hilma J. van der Horst,³ Margaret A. Lindorfer,⁴ Erika M. Cook,⁴ Jillian C. Tupitza,⁴ Clive S. Zent,⁵ Richard Burack,⁵ Karl R. VanDerMeid,⁵ Kristin Strumane,¹ Martine E. D. Chamuleau,³ Tuna Mutis,³ Rob N. de Jong,¹ Janine Schuurman,¹ Esther C. W. Breij,¹ Frank J. Beurskens,¹ Paul W. H. I. Parren,^{2,6} and Ronald P. Taylor^{4,†}

¹Genmab, Utrecht, The Netherlands; ²Department of Immunohematology and Blood Transfusion, Leiden University Medical Center, Leiden, The Netherlands; ³Department of Hematology, Amsterdam University Medical Center, Amsterdam, The Netherlands; ⁴Department of Biochemistry and Molecular Genetics, University of Virginia School of Medicine, Charlottesville, Virginia, USA; ⁵Wilmot Cancer Institute, University of Rochester Medical Center, Rochester, New York, USA; ⁶Lava Therapeutics, Utrecht, The Netherlands; [†]Corresponding author

Correspondence to: sio@genmab.com or rpt@virginia.edu

This PDF file includes:

Supplementary Methods and Materials

Supplementary Figures 1-6

Supplementary Table 1

Supplementary Methods and Materials

Cells

CLL cells were purified from the blood of newly diagnosed CLL patients (University of Rochester), in accordance with standard protocols (University of Rochester Institutional Review Board).¹ Bone marrow mononuclear cells (BMNCs), peripheral blood mononuclear cells (PBMCs) and lymph node suspension cells from patients with B-cell non-Hodgkin lymphoma (B-NHL, not otherwise specified (NOS)), follicular lymphoma (FL), marginal zone lymphoma (MZL) and mantle cell lymphoma (MCL) were obtained from the Amsterdam University Medical Center (Amsterdam, The Netherlands) after written informed consent and stored using protocols approved by the Privacy Review Board of the Netherlands Cancer Registry in accordance with the declaration of Helsinki. BMNCs and PBMCs were isolated by density-gradient centrifugation (Ficoll-Paque PLUS, GE Healthcare) from bone marrow aspirates or peripheral blood samples of lymphoma patients. Lymph node suspension cells were obtained by mechanical dissociation held overnight at 37°C and filtered using cell strainers. Cells were used in experiments directly or stored in liquid nitrogen until further use.

Reagents

Fluorescein isothiocyanate (FITC) conjugated rabbit anti-human C1q (Dako) was used for flow cytometry experiments. C1q depleted serum and purified human C1q were obtained from Quidel. Mouse anti-human IgM antibody HB57 and mouse anti-human IgG1 mAb HB43 were used as described.^{2, 3} Pooled normal human serum (NHS; AB positive) was obtained from Sanquin (Amsterdam, The Netherlands). mAbs labeled with Alexa dyes (A488, A555, A594, A647) were reacted with N-hydroxysuccinimidyl-esters following manufacturer's instructions (Molecular Probes).

Cell markers flow cytometry

Cell markers used to define cell populations from patients with B-cell lymphoma: CD45-KO (Beckman Coulter), CD19-PC7 (Beckman Coulter), CD3-V450 (BD), CD5-APC (BD), CD5-PE (Dako), CD10-APC-H7 (BD), CD10-PE (Dako), CD23-FITC (Biolegend), kappa-APC-H7 (BD), kappa-PE (Dako) and lambda-FITC (Emelca Bioscience). Within the CD45+ cell population, B cells were identified as CD3-CD19+ cells. Malignant cells were identified based on clonality by kappa/lambda staining (B-NHL (NOS), MZL). Tumor specific markers were used (when possible) depending on the lymphoma subtype: CD10+ (FL), CD5+CD23- (MCL).

Expression analysis

Expression levels of cellular markers were determined using an indirect immunofluorescence assay (QIFIKIT[®], Agilent Technologies) according to the manufacturer's instructions. Briefly, cells were labeled with primary mouse mAbs and incubated, in parallel with QIFIKIT[®] beads containing a defined number of mAb molecules, with FITC-labeled Polyclonal Goat Anti-Mouse

Immunoglobulins F(ab')₂. The number of antibody molecules per cell was determined by extrapolating the measured mean fluorescence intensity (MFI) to the calibration curve generated by plotting the MFI of the individual bead populations against the number of mAb molecules per bead.

Förster Resonance Energy Transfer (FRET) analysis

500,000 Daudi cells/well were incubated with 10 µg/mL A555-conjugated donor mAbs and/or 10 µg/mL A647-conjugated acceptor mAbs in 10 µL of RPMI/0.2% BSA in 96-well round-bottom plates for 15 minutes at 37°C. Cells were washed twice, pelleted by centrifugation (3 minutes, 300xg) and resuspended in 200 µL PBST. Mean fluorescence intensities (MFI) were determined by flow cytometry (FACS Canto II) by recording 10,000 events at 585/42 nm (FL2, donor A488) and ≥670 nm (FL3), both excited at 488 nm, and at 660/20 nm (FL4, acceptor A647), excited at 635 nm. Unquenched donor fluorescence intensity was determined with cells incubated with A555-conjugated donor mAbs, and non-enhanced acceptor intensity was determined with cells incubated with A647-conjugated acceptor mAbs. Proximity-induced FRET was determined by measuring energy transfer between cells incubated with A555-conjugated donor and A647-conjugated acceptor mAbs. MFI values allowed calculation of FRET according to the following equation:

Energy transfer (ET) = $FL3(D, A) - FL2(D, A)/a - FL4(D, A)/b$, wherein $a = FL2(D)/FL3(D)$, $b = FL4(A)/FL3(A)$, D is donor, A is acceptor and $FLn (D, A) = \text{donor} + \text{acceptor}$.⁴

ET values obtained were normalized:

Normalized energy transfer (%) = $100 * ET/FL3(D, A)$.

Synergy and colocalization analyses

Synergy between combinations of mAbs was determined using Loewe additivity-based combination index (CI) scores calculated by CompuSyn software (ComboSyn Inc., Paramus, NJ), whereby effects were categorized as additive (CI = 1), synergistic (CI < 1) or antagonistic (CI > 1).⁵ In brief, synergistic lysis exceeds the level of one mAb plus the predicted fractional lysis induced by the other mAb on the remainder of the cell population.

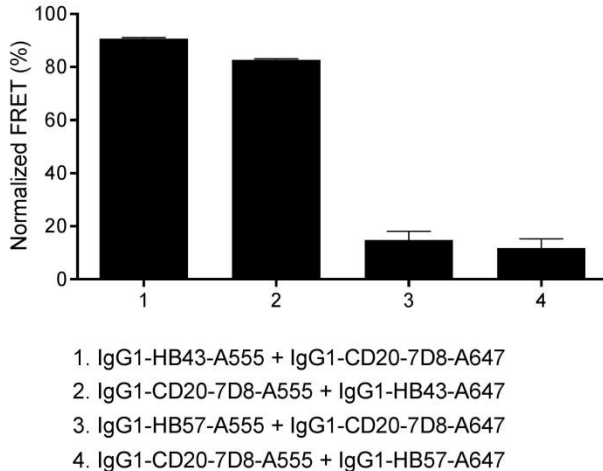
mAb colocalization was quantified by calculating spatial overlap (Manders' coefficients) between images of cell-bound A488-labeled Hx-CD20-7D8 and cell-bound A594-labeled Hx-CD37 using the colocalization plugin in ImageJ.^{6,7}

References

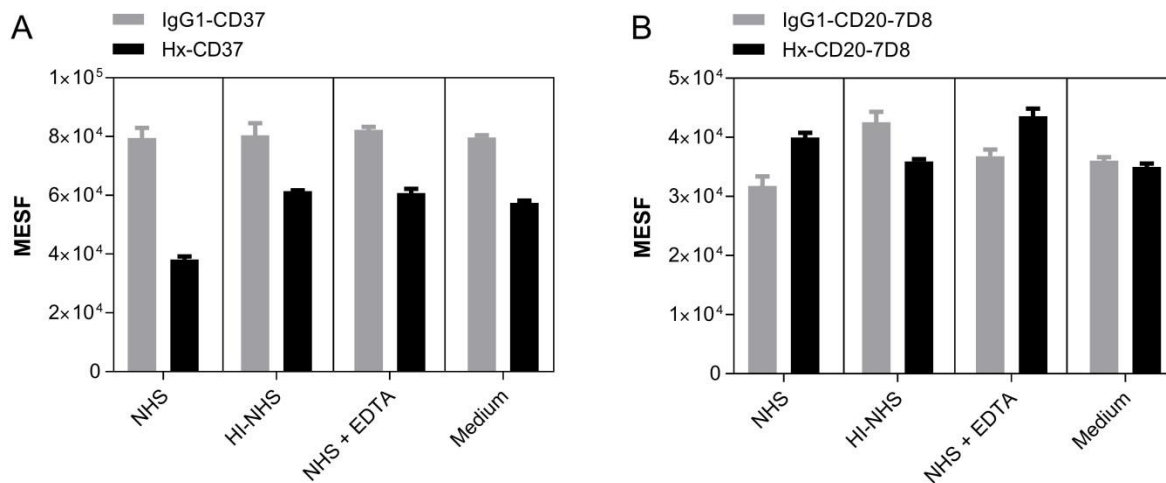
1. Baig NA, Taylor RP, Lindorfer MA, et al. Complement dependent cytotoxicity (CDC) in chronic lymphocytic leukemia (CLL): Ofatumumab enhances alemtuzumab CDC and reveals cells resistant to activated complement. *Leuk Lymphoma*. 2012;53(11):2218-2227.
2. Kennedy AD, Beum PV, Solga MD, et al. Rituximab Infusion Promotes Rapid Complement Depletion and Acute CD20 Loss in Chronic Lymphocytic Leukemia. *J Immunol*. 2004;172(5):3280.

3. Taylor RP, Wright EL, Pocanic F. Quantitative analyses of C3b capture and immune adherence of IgM antibody/dsDNA immune complexes. *J Immunol.* 1989;143(11):3626.
4. Cragg MS, Morgan SM, Chan HTC, et al. Complement-mediated lysis by anti-CD20 mAb correlates with segregation into lipid rafts. *Blood.* 2003;101(3):1045.
5. Chou T-C. Theoretical Basis, Experimental Design, and Computerized Simulation of Synergism and Antagonism in Drug Combination Studies. *Pharmacol Rev.* 2006;58(3):621.
6. Schneider CA, Rasband WS, Eliceiri KW. NIH Image to ImageJ: 25 years of image analysis. *Nat Methods.* 2012;9(6):71.
7. Manders E. M M, Verbeek F J, Aten J A. Measurement of co-localization of objects in dual-colour confocal images. *JMic.* 1993;169(3):375-382.

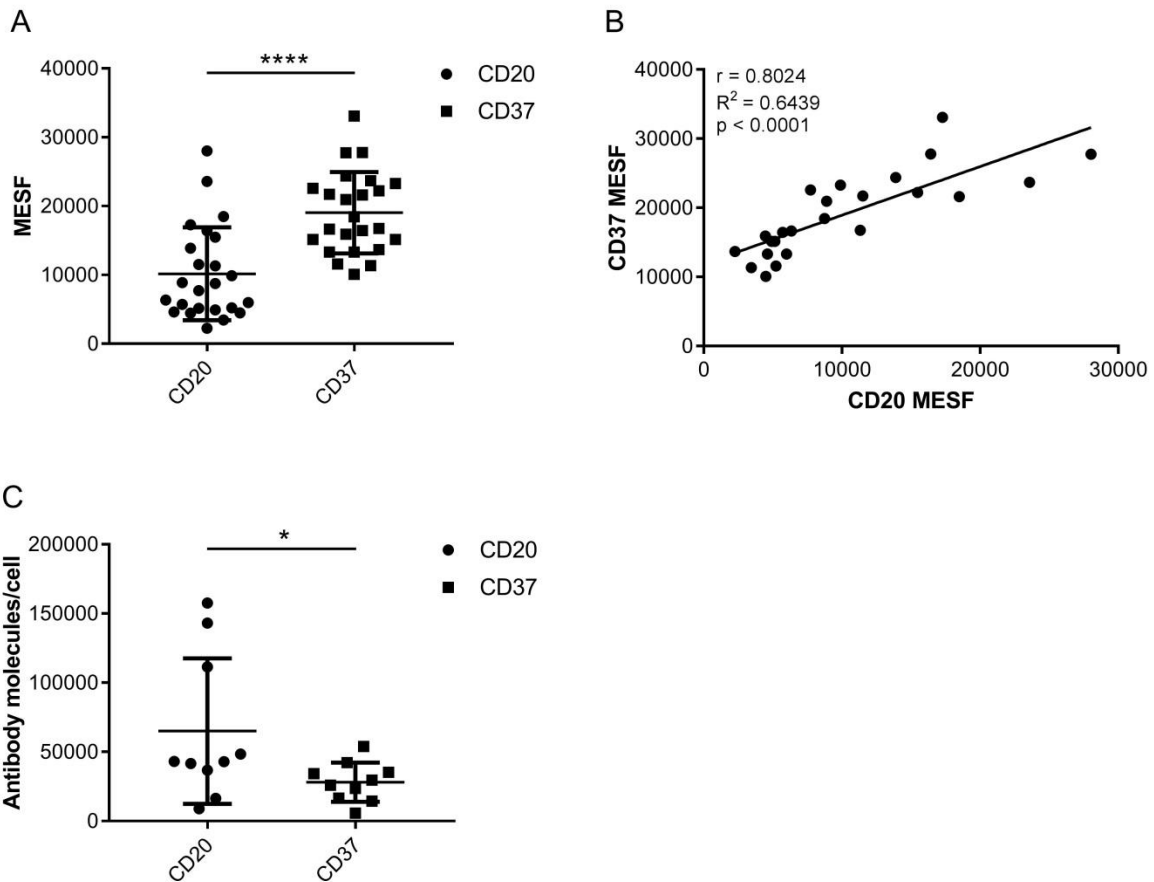
Supplementary Figures and Tables



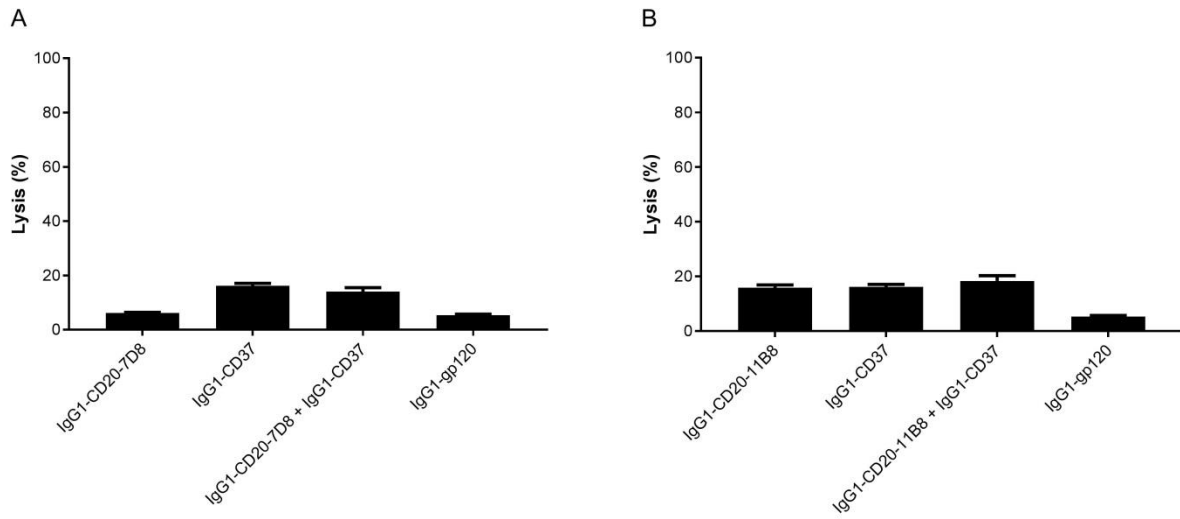
Supplementary Figure 1. Evaluation of the dynamic range of fluorescence resonance energy transfer (FRET) detection determined by flow cytometry using control mAbs. Daudi cells were incubated with 10 $\mu\text{g}/\text{mL}$ of A555- or A647-conjugated CD20 mAb 7D8 (IgG1-CD20-7D8) and washed, followed by 10 $\mu\text{g}/\text{mL}$ A555- or A647-conjugated mouse-anti-human IgG1 mAb HB43 (IgG1-HB43; positive control) or mouse-anti-human IgM mAb HB57 (IgG1-HB57; negative control) for 15 minutes at 37°C. FRET was calculated from MFI values as determined by flow cytometry. Data shown are mean and SD of six replicates collected from three independent experiments. IgG1-HB43 was used as a positive control for proximity-induced FRET by virtue of its ability to directly bind, and thus colocalize with a human IgG1 mAb, such as the WT CD20 mAb 7D8 on the cell surface. As binding of A555- or A647-conjugated HB43 requires a cell surface-bound IgG1 mAb, unconjugated IgG1-CD20-7D8 was used for primary binding in the single stainings (calculating the unquenched donor and non-enhanced acceptor fluorescence intensities) and A555- or A647-conjugated IgG1-CD20-7D8 mAb was used for primary binding in the combination stainings (calculating energy transfer efficiency). Using the same setup, IgG1-HB57 was used as a negative control for proximity-induced FRET. HB57 is a murine mAb that binds membrane-bound human IgM (B-cell receptor) on Daudi cells, and was expected to poorly colocalize with the human antibody IgG1-CD20-7D8. Conjugated IgG1-CD20-7D8 and IgG1-HB43 efficiently colocalized with an energy transfer efficiency of 90%, while IgG1-CD20-7D8 and IgG1-HB57 poorly colocalized with ~10% energy transfer efficiency. These data validated the flow cytometry FRET analysis to assess antibody colocalization using A555- and A647-conjugated antibodies.



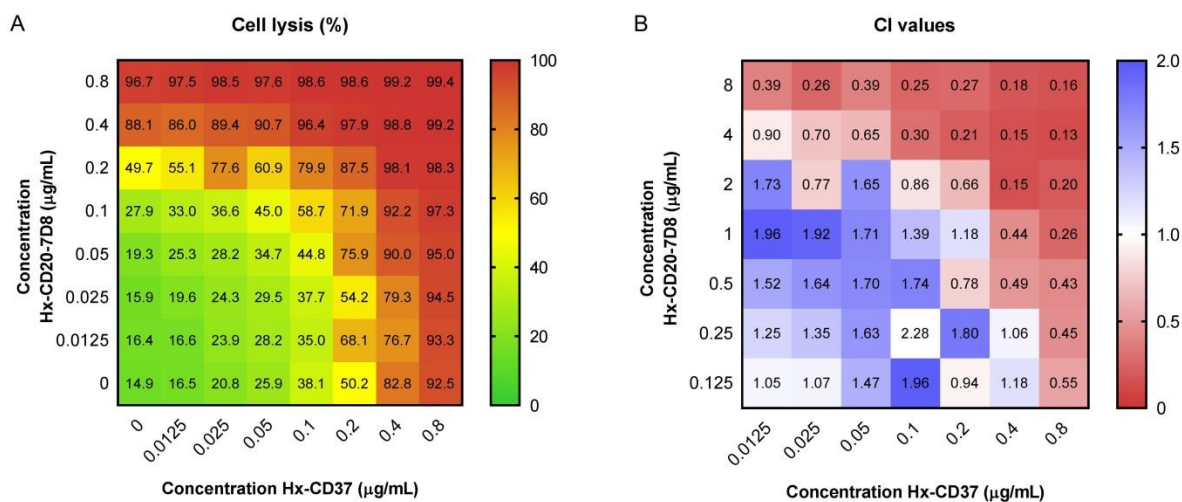
Supplementary Figure 2. Binding of CD20 and CD37 mAbs to tumor B cells obtained from a patient diagnosed with CLL (patient A). Antibody binding on primary CLL B cells was analyzed using 16 $\mu\text{g}/\text{mL}$ WT CD37 mAb 37.3 (IgG1-CD37) and its hexamerization-enhanced variant Hx-CD37 (A) or WT CD20 mAb 7D8 (IgG1-CD20-7D8) and its hexamerization-enhanced variant Hx-CD20-7D8 (B) in the presence NHS, HI-NHS, NHS + EDTA or medium. Binding was detected using A488-conjugated mouse anti-human IgG1 Fc mAb HB43 and mean fluorescence intensities were converted to molecules of equivalent soluble fluorochrome (MESF) using calibrated beads (Spherotech). Representative examples of three replicate experiments are shown.



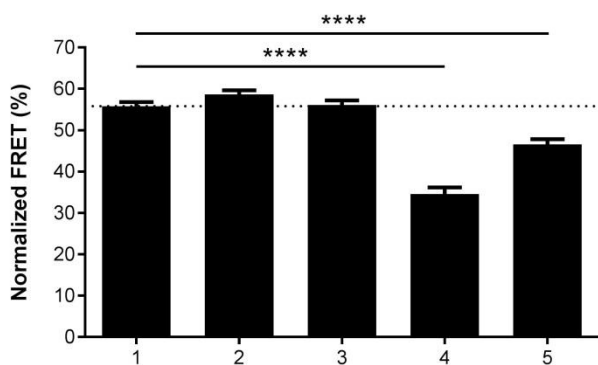
Supplementary Figure 3. CD20 and CD37 target expression levels on tumor B cells obtained from patients with B-cell malignancies. (A) CD20 and CD37 expression. Binding was detected using an A488-conjugated mouse anti-human IgG1 Fc mAb HB43 and mean fluorescence intensities were converted to molecules of equivalent soluble fluorochrome (MESF) using calibrated beads (Spherotech). (B) Correlation analysis of CD20 and CD37 expression levels on tumor B cells from 24 CLL patient samples described in (A). The Pearson's correlation coefficient (r and R^2) was calculated using GraphPad Prism software. (C) CD20 and CD37 expression levels on tumor B cells of 2 B-NHL (NOS), 3 FL, 2 MZL and 3 MCL patient samples. Expression levels were determined using a human IgG calibrator kit (Agilent Technologies). The number of antibody molecules per cell was calculated from the antibody-binding capacity (mean fluorescence intensity) normalized to a calibration curve, according to the manufacturer's guidelines. Significant differences are indicated as * $p < 0.05$ and **** $p < 0.0001$.



Supplementary Figure 4. Minimal cell lysis observed in assays with heat-inactivated serum indicates that cell killing is complement dependent. Daudi cells opsonized with 30 $\mu\text{g}/\text{mL}$ WT type I CD20 mAb 7D8 (IgG1-CD20-7D8) (A) or WT type II CD20 mAb 11B8 (IgG1-CD20-11B8) (B), anti-CD37 mAb 37.3 (IgG1-CD37), or a combination thereof (15 + 15 $\mu\text{g}/\text{mL}$) for 45 minutes at 37°C in the presence of 20% heat-inactivated NHS. HIV gp120-specific mAb b12 (IgG1-gp120) was used as a negative control human mAb. Cell kill is expressed as the percentage lysis determined by the fraction of PI-positive cells. Representative examples of two replicates are shown.



Supplementary Figure 5. (A) 8 x 8 CDC dose response matrix plot for the combination of hexamerization-enhanced CD37 mAb Hx-CD37 (0-0.8 µg/mL) with hexamerization-enhanced CD20 mAb Hx-CD20-7D8 (0-0.8 µg/mL) tested on Daudi cells and categorized as a color gradient from green (0% lysis) to yellow (50% lysis) to red (100% lysis). HIV gp120-specific mAb b12 (IgG1-gp120) was used as a negative control human mAb. (B) Loewe additivity-based Combination index (CI) values calculated by CompuSyn for the CDC dose response matrix as described in (A) and categorized as synergistic (<1, red), additive (1, white) and antagonistic (>1, blue). Representative examples of two replicate experiments are shown. CDC induction is expressed as the percentage lysis determined by the fraction of PI-positive cells.



1. Hx-CD37-A555 + Hx-CD20-11B8-A647
2. Hx-CD37-K439E-A555 + Hx-CD20-11B8-S440K-A647
3. Hx-CD37-S440K-A555 + Hx-CD20-11B8-K439E-A647
4. Hx-CD37-K439E-A555 + Hx-CD20-11B8-K439E-A647
5. Hx-CD37-S440K-A555 + Hx-CD20-11B8-S440K-A647

Supplementary Figure 6. The effect of introducing Fc-Fc inhibiting mutations S440K and K439E on the molecular proximity of hexamerization-enhanced CD20 and CD37 mAbs on the cell membrane of Daudi cells. Daudi cells were incubated with 10 µg/mL A555-conjugated hexamerization-enhanced CD37 mAb 37.3 (Hx-CD37) variants and 10 µg/mL A647-conjugated hexamerization-enhanced CD20 mAb 11B8 (Hx-CD20-11B8) variants for 15 minutes at 37°C. FRET was calculated from MFI values as determined by flow cytometry. Data shown are mean and SD of six replicates collected from three independent experiments.

Supplementary Table 1. Average Loewe-additivity-based combination index (CI) values calculated by CompuSyn at different effective doses of a CDC dose-response matrix using combinations of hexamerization-enhanced CD20 mAb Hx-CD20-7D8 or Hx-CD20-11B8 with hexamerization-enhanced CD37 mAb Hx-CD37.

Antibody Combination	CI values* at different effective doses (ED):			
	ED50	ED75	ED90	ED95
Hx-CD20-7D8 + Hx-CD37	0.96	0.66	0.47	0.37
Hx-CD20-11B8 + Hx-CD37	0.72	0.52	0.39	0.31

*CI values can be categorized as synergistic (<1), additive (=1) and non-synergistic (>1).